

000 001 002 003 004 005 DAMO: DATA MIXING OPTIMIZER IN FINE-TUNING 006 MULTIMODAL LLMs FOR MOBILE PHONE AGENTS 007 008 009

010 **Anonymous authors**
011 Paper under double-blind review
012
013
014
015
016
017
018
019
020
021
022
023
024
025
026
027
028
029
030

ABSTRACT

031 Mobile Phone Agents (MPAs) have emerged as a promising research direction
032 due to their broad applicability across diverse scenarios. While Multimodal Large
033 Language Models (MLLMs) serve as the foundation for MPAs, their effectiveness
034 in handling multiple mobile phone tasks simultaneously remains limited. Although
035 multitask supervised fine-tuning (SFT) is widely adopted for multitask learning,
036 existing approaches struggle to determine optimal training data compositions for
037 peak performance. To address this challenge, we propose DaMo (Data Mixture
038 Optimizer) – a novel solution employing a trainable network that predicts optimal
039 data mixtures by forecasting downstream task performance for any given dataset
040 ratio. To support comprehensive evaluation, we introduce PhoneAgentBench, the
041 first specialized benchmark to evaluate MLLMs on multimodal mobile phone tasks,
042 comprising 1,235 QA pairs spanning diverse real-world industrial mobile applica-
043 tion scenarios. Demonstrating strong predictive capability ($R^2=0.81$) in small-scale
044 pilot experiments, DaMo efficiently extrapolates optimal data mixing configura-
045 tions. Our results show DaMo achieves a 3.38% performance improvement on
046 PhoneAgentBench compared to alternative methods. Furthermore, extensive ex-
047 periments across established benchmarks including BFCL-v3, MME-Reasoning,
048 MME-Perception, and OCRBench reveal DaMo’s superior generalization, outper-
049 forming other approaches by 2.57% in terms of average score. When used solely for
050 MLLM optimization on the BFCL-v3 task, DaMo improves the metrics by 12.47%
051 than other methods. Notably, DaMo maintains robust scalability, preserving its
052 effectiveness when applied to other model architectures.
053

1 INTRODUCTION

034 Mobile phone agents (MPAs) have attracted huge attention due to their practicability in a multitude of
035 scenarios. An ideal MPA has to master multiple capabilities, such as environment perception Zhang
036 et al. (2024); Ingold (2021), task planning Song et al. (2023); Liu et al. (2024b), multimodal
037 reasoning Lu et al. (2022); Wang et al. (2024), function call Chen et al. (2024a); Basu (2024), and
038 personalized memory Li et al. (2024a); Yuan et al. (2023).
039

040 The advent of multimodal large language models (MLLMs) provides a promising solution for the
041 ideal agent. However, existing MLLMs encounter significant challenges in effectively integrating
042 these diverse capabilities. Consequently, developing a versatile model capable of handling multiple
043 tasks is critical for creating a advanced phone agent.
044

045 Multitask supervised fine-tuning (SFT) is the predominant approach utilized to empower MLLMs in
046 addressing multiple tasks. Nevertheless, in light of numerous training datasets and downstream tasks,
047 identifying optimal data blending strategies to maximize model performance remains a significant
048 research challenge. The existing works on data mixture optimization Xie et al. (2023b); Ge et al.
049 (2024); Albalak et al. (2023) focus on the pretraining phase by predicting validation loss. However,
050 these methods are inadequate to determine the optimal data mixture for multitask SFT, as they fail to
051 directly correlate with model performance on downstream tasks.
052

053 We investigate whether downstream task performance can be reliably predicted for any given data
054 mixture prior to actual model training, including identifying the optimal mixture that would yield
055 optimal performance. To this end, we propose the **downstream task performance prediction** (DaPP)
056 method to build **Data Mixing Optimizer** (DaMo). DaPP leverages a function to straightly predict
057

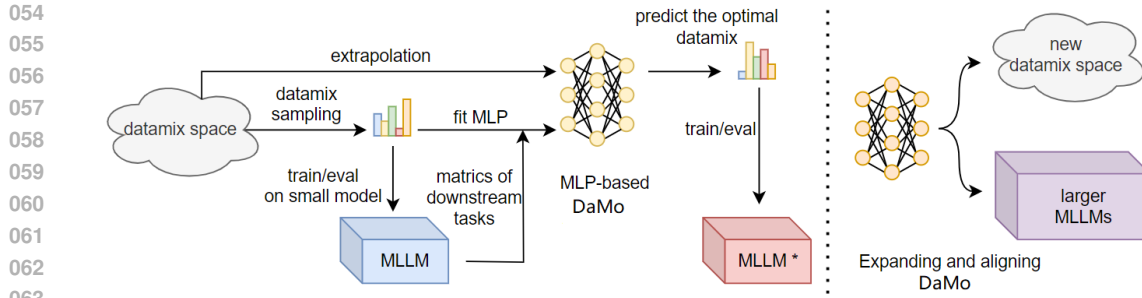


Figure 1: Illustration of our pipeline for obtaining the optimal data mixture. Left: Given m training sets with a batch size of b , all possible mixture combinations constitute the data mixing space. We sample a small number of data mixture from this space, train them on a small MLLM, and then evaluate downstream task performance. Using the data mixture as inputs and the metrics as outputs, we fit a MLP to establish the DaMo. By extrapolating from the data mixing space, we predict the optimal data mixture to train the MLLM. Right: Demonstrates the extension and alignment of DaMo to other MLLMs and new data mixing spaces.

model performance at downstream tasks. Considering that exponential functions used in Xie et al. (2023b); Ge et al. (2024); Albalak et al. (2023) are not well-aligned with SFT performance trajectories for specific downstream applications Huang et al. (2019); Xie et al. (2024); Isik et al. (2024), we propose to utilize a trainable neural network for target fitting. The optimal data mixture is obtained through extrapolation via DaMo, with the process shown in Fig. 1.

Another obstacle in developing an ideal mobile phone agent is the absence of comprehensive real-world industrial benchmarks for evaluating MPA performance. Current benchmarks Gao et al. (2024); Cheng et al. (2024); Li et al. (2025); Wang et al. (2025) in this domain predominantly focus on Graphical User Interface (GUI) tasks, which fail to capture the full spectrum of practical application scenarios. To address this critical gap, we introduce PhoneAgentBench - a thorough benchmark encompassing four fundamental capabilities: 1) complex task planning, 2) device-native tool usage, 3) multimodal memory, and 4) screen context understanding. Our benchmark comprises 2,350 meticulously validated test cases that simulate real-world phone interactions, with 55% necessitating the simultaneous activation of more than 3 tools.

Our proposed DaMo demonstrates three key advantages. First, it achieves 3.38% average performance gain on PhoneAgentBench compared to state-of-the-art method, DML Ye et al. (2024). Second, when evaluated on the general benchmarks including BFCL-v3 Yan et al. (2024), MME-perception Fu et al. (2023), MME-reasoning Yuan et al. (2025), and OCRBench Liu et al. (2024c), DaMo outperforms DML by 2.57% in terms of average score. Third, DaMo exhibits robust scalability—Pearson correlations between predicted and actual scores remaining consistently high (0.75~0.95) across other models, while introducing significant gains on downstream tasks over other methods.

Our core contributions are as follows.

- We propose Downstream Task Performance Prediction method to establish a Data Mixing Optimizer, which directly estimates model performance on downstream tasks for optimal data mixing.
- We construct PhoneAgentBench, a benchmark spanning four critical dimensions: complex task planning, device-native tool usage, multimodal memory, and screen context understanding, mirroring real-world mobile interaction scenarios.
- Through systematic experiments, our method demonstrates exceptional generalization and scalability, outperforming other methods on PhoneAgentBench, and achieving state-of-the-art performance on the BFCL-V3 leaderboard among 4B-scale models, while also maintaining stable prediction accuracy with efficient adaptation to other models.

108
109
110 Table 1: PhoneAgentBench
111
112
113

Dataset	Evaluation ability	Data size	Dataset	Evaluation ability	Data size
MT-Plan	Mulitmodal Task Planning	100	MM-RR	Multimodal Reference Resolution	130
ACU	Agent Context Understand	100	MM-NER	Multimodal Named Entity Recognition	376
APP-Rec	APP Recognition	100	Mobile-FC	Mobile Function Calling	429

144
145
146 2 RELATED WORK
147
148

149 **Data Mixing** Data mixtures follow distinct optimization paths in pre-training versus fine-tuning.
 150 Current research can be broadly divided into two paradigms. For pre-training, methods optimize
 151 language model perplexity (PPL). Early heuristic approaches like uniform sampling Michel et al.
 152 (2021) gave way to learnable solutions; DoReMi Xie et al. (2023a) uses Group DRO Sagawa
 153 et al. (2020) for domain weights; ODM Albalak et al. (2023) frames selection as a bandit problem;
 154 BiMix Ge et al. (2024) jointly optimizes domain proportions and data scaling. All these PPL-focused
 155 approaches differ fundamentally from fine-tuning objectives.

156 Fine-tuning research remains limited: industrial solutions (LLaMA3 Grattafiori et al. (2024), Tulu3
 157 Lambert et al. (2024)) rely on costly manual iteration; SFTMix Xiao et al. (2024) optimizes intra-
 158 dataset ratios but cannot handle multi-source data; MoE-based methods Zhu et al. (2024) adjust
 159 weights but lack interpretable criteria. Key gaps remain in developing general multi-source mixing
 160 schemes and theoretical guidance for fine-tuning datasets.

161
162 **Agent Benchmark** Recent advancements in agent-based systems have spurred various benchmarks
 163 to evaluate their capabilities. PlanBench Valmeekam et al. (2023) and REALM-Bench Geng &
 164 Chang (2025) assess planning capabilities. ToolBench Qin et al. (2023), BFCL Yan et al. (2024), and
 165 API-Bank Li et al. (2023) evaluate tool invocation and ReflectionBench Li et al. (2024b) measures self-
 166 reflection. LTM Benchmark Castillo-Bolado et al. (2024) tests memory retention. These benchmarks
 167 are limited to single-dimensional evaluations, lacking holistic assessment. GAIA Mialon et al. (2023)
 168 uses end-to-end evaluation to assess general agents, but lacks granularity. AgentBench Liu et al.
 169 (2023) and KAgentBench Pan et al. (2023) are unimodal, ignoring multimodal interaction. Moreover,
 170 all of these benchmarks deviates from real-world phone scenarios. ScreenSpot-Pro Cheng et al.
 171 (2024), MobileViews Gao et al. (2024), VisualAgentBench Liu et al. (2024a), ScreenSpot-Pro Li et al.
 172 (2025), and MMBench-GUI L2 Wang et al. (2025) can evaluate phone agents, but they are designed
 173 mainly for GUI tasks in mobile scenarios. A critical gap remains: the absence of a comprehensive
 174 benchmark supporting multimodal interaction while systematically evaluating mobile phone agents
 175 across planning, tool usage, memory, and other dimensions. This hinders iterative optimization and
 176 underscores our work’s innovation potential.

177
178 3 PHONEAGENTBENCH
179
180

181 Current open-source agent evaluation benchmarks Valmeekam et al. (2023); Li et al. (2024b); Liu
 182 et al. (2023); Geng & Chang (2025) are unable to assess agents for tackling multimodal tasks in
 183 mobile phone scenarios. Mobile Phone agent relevant benchmarks Gao et al. (2024); Cheng et al.
 184 (2024); Li et al. (2025); Wang et al. (2025) primarily evaluate the GUI tasks of MLLMs. However,
 185 they lack support for multimodal interaction and do not provide systematic evaluation across key
 186 dimensions such as planning, tool use, and memory. This mismatch with mobile phone agent
 187 scenarios poses a significant challenge. To address this gap, we aim to develop a benchmark tailored
 188 to real-world industrial application scenarios, thereby accelerating the practical implementation of
 189 agent technology.

190 We develop a novel benchmark suite specifically designed for mobile phone agents. This suite
 191 encompasses six carefully curated datasets focusing on key mobile phone application tasks, thereby
 192 offering a holistic assessment of phone agents’ performance across diverse capabilities critical to
 193 real-world mobile applications. Details of the tasks are provided in Table 1. We describe the data
 194 construction process using the Multimodal Task Planning task (MT-Plan) as a case in point.

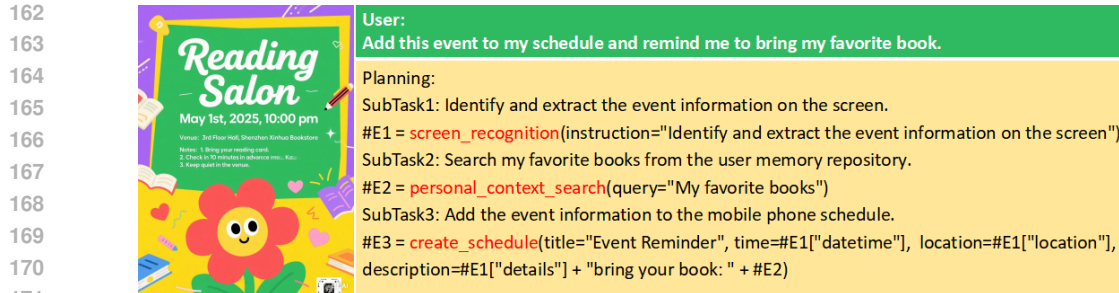


Figure 2: MT-Planning example

MT-Plan MT-Plan is designed to evaluate multimodal task planning capabilities. Unlike T-Eval planning Chen et al. (2023), it focuses on multimodal complex task interactions in phone agent scenarios. As shown in Fig.2, MT-Plan takes \langle image + query \rangle as input and outputs a planning structured as a directed acyclic graph (DAG). Images are sourced from real photos or mobile screenshots, while tools are derived from APIs provided by operating systems or app ecosystems. Queries and plannings are carefully constructed by annotators based on the images. Queries are required to be concise, colloquial, and aligned with real users' daily needs. Meanwhile, tasks must be sufficiently complex to require plannings to invoke at least 2 tools. To ensure data accuracy, three annotators were invited to conduct cross-validation. Additionally, to evaluate the dataset's complexity and diversity, we compared the metrics of MT-Plan and T-Eval planning, as presented in Table 7.

The MT-Plan evaluator adopts the T-Eval planning evaluator Chen et al. (2023): it compares the predicted plan with the golden plan, and calculates the score based on the length of the longest ordered action sequence derived from similarity-matched pairs.

The construction methods of the remaining five datasets are presented in AppendixA.2.

4 METHODOLOGY

This section formalizes multitask fine-tuning optimization as identifying the optimal data mixture to maximize downstream task metrics. We propose predicting unseen mixture performance by fitting the performance of downstream tasks with limited training configurations. Analysis of single and dual dataset experiments demonstrates why exponential/power-law functions fail to model convergence patterns, prompting our neural network solution for extrapolating optimal data mixture.

4.1 PROBLEM FORMULATION

Consider fine-tuning a MLLM using a mixture of m heterogeneous training datasets, denoted as $\mathcal{D} = \cup_{i=1}^m \mathcal{D}_i$. Each \mathcal{D}_i contains n_i labeled samples with the total number of samples being $N = \sum_{i=1}^m n_i$. We fine-tune the MLLM starting from initial parameters θ_0 , using a batch size b , for a maximum of $T = \lceil N/b \rceil$ training steps.

We define the **data mixture proportion** as $\mathbf{p} = [p_1, p_2, \dots, p_m]$, where p_i represents the proportion of samples drawn from dataset \mathcal{D}_i . The data mixture proportion \mathbf{p} satisfies $\sum_{i=1}^m p_i = 1$.

Similarly, we consider k downstream test datasets, denoted as $\mathcal{D}^{test} = \cup_{j=1}^k \mathcal{D}_j^{test}$. Let $\mathbf{s} = [s_1, \dots, s_k] \in [0, 1]^k$ represent the score of each test dataset. The overall average score of the MLLM with parameters θ is given by $S_\theta = \frac{1}{k} \sum_{j=1}^k s_j$.

We aim to find the optimal data mixture proportion $\mathbf{p}^* \in \mathcal{P}$ (where \mathcal{P} denotes the complete data mixing space, $\mathbf{p} \in \mathbb{R}^m$) that maximizes the overall average score of downstream tasks:

$$\mathbf{p}^* = \arg \max_{\mathbf{p} \in \mathcal{P}, t \leq T} \mathbb{E}_{\theta \sim \mathcal{A}(\mathbf{p}, t, \theta_0)} S_\theta \quad (1)$$

216 where \mathcal{A} denotes the fine-tuning process that produces the MLLM’s parameters θ based on the initial
 217 parameters θ_0 for t steps using the data mixture strategy \mathbf{p} .
 218

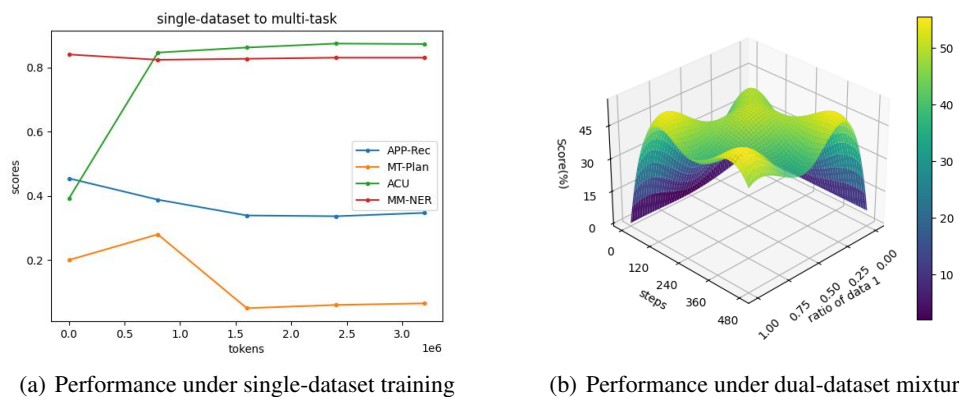
219 Without any constraints, the size of the set \mathcal{P} that represents batch-wise permutations is given
 220 by $|\mathcal{P}| = \frac{N!}{(b!)^T}$, which is computationally intractable. Therefore, we introduce some necessary
 221 assumptions to prune the space \mathcal{P} . By disregarding the order of samples within the same dataset and
 222 keeping the data mixture fixed throughout the entire number of training steps T , we obtain a smaller
 223 data mixing space \mathcal{P}_{fix} . According to the principle of combination with repetition, the size of this
 224 fixed data mixing space \mathcal{P}_{fix} is given by $|\mathcal{P}_{fix}| = C_{m+b-1}^m$.
 225

226 4.2 PERFORMANCE PREDICTION OF DOWNSTREAM TASKS

227 We aim to find the optimal mixture $\mathbf{p}^* \in \mathcal{P}$. Given the high training cost of MLLMs, an exhaustive
 228 brute-force search is clearly impractical. To address this problem, we propose DaMo which is able to
 229 estimate model performance at downstream tasks without training, given any mixture proportions of
 230 training data. Towards this target, we fit a function f to predict performance based on data mixtures.
 231 To obtain accurate f , an efficient sampling approach is proposed to generate training samples. The
 232 sampling process is detailed as: 1) Randomly select a small set of m -dimensional mixing ratios
 233 from \mathcal{P}_{fix} . 2) Train MLLM while saving checkpoints at every τ steps. 3) Evaluate each checkpoint
 234 to obtain the performance of downstream tasks. This process yields the mapping: (data mixture,
 235 training steps) \rightarrow performance of downstream tasks. Based on these samples, we fit f to predict the
 236 performance trajectory of unseen mixture:
 237

$$\hat{\mathbf{s}} = f(\mathbf{p}, t; \theta_0), \quad (2)$$

240 where θ_0 is initial model state and $t = \tau * i$ is train steps of the i -th checkpoint. With an accurate
 241 fitting of f , we can extrapolate performance estimates across the entire \mathcal{P}_{fix} space, dramatically
 242 reducing the model training costs required to identify the optimal data mixture.
 243
 244



255
 256 Figure 3: Training dynamics on downstream tasks
 257
 258

261 The critical challenge lies in selecting an appropriate function f . While conventional exponential or
 262 power-law functions Achiam et al. (2023); Grattafiori et al. (2024) are widely adopted for pretraining
 263 loss convergence, we hypothesize their inadequacy in multi-task fine-tuning scenarios involving
 264 interacting datasets. To validate this, we systematically analyze training dynamics under two configu-
 265 rations: (1) single-dataset training (MultiModal-Understanding, MMU) and (2) dual-dataset mixtures
 266 (APP Recognition (APP-Rec) + MMU, see Section 5.1).
 267

268 We trained a MLLM on the MMU dataset and evaluated its performance on PhoneAgentBench.
 269 As shown in Fig. 3(a), the results reveal distinct task-specific patterns: (1) **Enhancement**: MMU
 270 significantly improves ACU performance. (2) **Conflict**: APP-Rec performance degrades with MMU
 271 training steps. (3) **Neutrality**: MM-NER shows no correlation with MMU training. (4) **Overfitting**:

270 MT-Plan exhibits initial gains followed by sharp declines, indicating harmful overfitting beyond
 271 optimal data volume.
 272

273 Fig. 3(b) demonstrates the complex interaction when training on the mixed dataset of APP-Rec
 274 and MMU for the APP-Rec task. The 3D performance surface (X: training steps, Y: APP-Rec
 275 training dataset ratio, Z: APP-Rec bench score) exhibits **non-convex topology with non-monotonic**
 276 **fluctuations** along both axes. This nonlinearity fundamentally prevents analytical solutions for Eq. 1
 277 and invalidates conventional exponential and power functions.
 278

278 Motivated by neural networks’ capacity to model high-dimensional nonlinearities, we pioneer their
 279 application to DaMo. Our framework implements f as a multi-layer perceptron (MLP) that directly
 280 maps data mixture and training step to task performance:
 281

$$\hat{s} = f_{MLP}(\mathbf{p}, t; \theta_0), \quad (3)$$

283 4.3 OPTIMAL DATA MIXTURE EXTRAPOLATION

285 When we define the data mixture space as \mathcal{P}_{fix} and employ MLP as the fitting function, the
 286 optimization objective in Eq. 1 can be reformulated as follow.
 287

$$\mathbf{p}_{fix}^* = \arg \max_{\mathbf{p} \in \mathcal{P}_{fix}, t \leq T} \frac{1}{k} \sum_{j=1}^k f_{MLP}^j(\mathbf{p}, t; \theta_0). \quad (4)$$

291 Where j denotes j th downstream task. Given the negligible inference cost of MLP models, DaMo can
 292 efficiently extrapolate the optimal data mixture. We first iterate through all possible data mixtures in
 293 the \mathcal{P}_{fix} space to predict downstream task performance scores. Subsequently, we sort these predicted
 294 scores and select the top- k highest-scoring mixtures to train our MLLM. This approach enables us to
 295 systematically identify the optimal data mixture without exhaustive empirical testing. The complete
 296 algorithm pseudocode is provided in Appendix B.
 297

298 5 EXPERIMENTS

300 5.1 EXPERIMENTS SETTINGS

302 **Training datasets** Our training data corpus integrates 12 open-source and self-built datasets,
 303 encompassing both Chinese and English languages. The comprehensive dataset contains a total of
 304 220K instructions, providing a diverse and extensive resource for our model training. Details are
 305 provided in Appendix A.3

307 **Downstream Task Evaluation** Besides PhoneAgentBench, we further evaluated our method on
 308 four widely used open-source benchmarks to verify generalization, including BFCL-V3 Yan et al.
 309 (2024), MME-perception Fu et al. (2023), MME-reasoning Yuan et al. (2025) and OCRBench Liu
 310 et al. (2024c). These benchmarks collectively encompass a total of ten evaluation tasks, and all
 311 metrics are expressed as percentages (0-100%), with higher values indicating superior performance.
 312

313 **Baseline** We selected two heuristic approaches commonly used in industry and one representative
 314 loss-based exponential fitting method: **Uniform Mixture**: All datasets are sampled with equal
 315 weights. **Natural Mixture**: Sampling weights are proportional to the size of each dataset. **Data**
 316 **Mixing Laws (DML)** Ye et al. (2024): An exponential function-based loss fitting method to predict
 317 the optimal mixture.
 318

319 **Implement Details** We conducted a series of experiments to verify the effectiveness of DaMo.
 320 Initially, we performed training and evaluation based on InternVL2.5-4B Chen et al. (2024b) to
 321 obtain fitting samples (in the format of (\mathbf{p}, t, s)) for a two-layer MLP training. Subsequently, we
 322 calculated the coefficient of determination (R^2) Wright (1921) via 10-fold cross-validation to verify
 323 the fitting performance. Then, we used the MLP to predict the downstream task performance of
 324 unseen data mixtures and train MLLM on the optimal data mixture. Finally, we verified the scalability
 325 of DaMo on other models. Additional implement details are available in Appendix A.1.
 326

324 5.2 FITTING SCORE OF NEURAL NETWORK
325

326 As analyzed theoretically for \mathcal{P}_{fix} in Section 4.1, when the number of training datasets $m = 12$ and
327 batch size $b = 16$, \mathcal{P}_{fix} forms a discrete enumerable space with a size of $\binom{12+16-1}{12} \approx 1.7 \cdot 10^7$. This
328 is a fairly large space, so how many sample points does DaMo need to fit the entire \mathcal{P}_{fix} well? We
329 gradually increased the number of training sample points for the MLP, and as shown in Table 2, when
330 the number reaches 250, the fitting score of the MLP gradually converged. Considering the training
331 cost, we stopped further experiments. Notably, 250 samples account for only a negligible portion of
332 the entire \mathcal{P}_{fix} space, yet they enable $R^2 = 0.81$ in 10-fold cross-validation. This indicates that the
333 performance of MLLM on downstream tasks has an inherent connection with the characteristics and
334 mixing patterns of training data, and DaMo learns this mapping via neural networks.
335

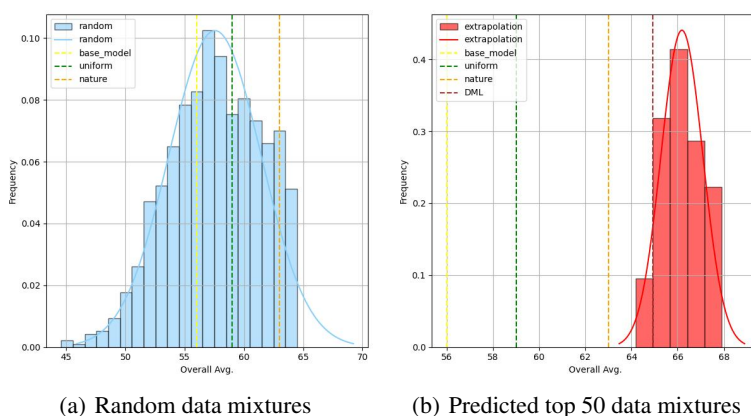
336 Table 2: MLP fitting dynamics

337 Number of fitting samples	338 Cost of getting samples (H20-hours)	339 Score (R^2)
339 50	340 872	341 0.58
340 100	341 1817	342 0.57
341 150	342 2581	343 0.74
342 200	343 3521	344 0.78
343 250	344 4225	345 0.81

344 5.3 DOWNSTREAM TASK PERFORMANCE OF UNSEEN DATA MIXTURES
345

346 We commence with a systematic analysis of the sample point distribution. As shown in Fig. 4(a),
347 the score distribution under random data mixtures approximately follows a normal distribution,
348 revealing two critical characteristics: (1) The absence of a right-side long tail indicates that excellent
349 data mixtures are extremely sparse. (2) The performance of random mixture is predominantly
350 mediocre, and baseline methods (vertical dashed line) show no discernible advantage, demonstrating
351 the inefficiency of heuristic approaches.
352

353 We used DaMo to predict across \mathcal{P}_{fix} space, selected the top 50 data mixtures with the best predicted
354 performance, and conducted actual training and evaluation on MLLM. The distribution of their
355 performance is shown in Fig. 4(b), DaMo successfully identifies data mixtures with significantly
356 higher overall average scores compared to baseline methods.
357

372 Figure 4: Probability distributions of overall average scores across different checkpoints.
373

374 Through selecting mixture with top 1 predicting score on PhoneBenchAgent and open-source benchmarks
375 to train MLLM, we obtain the performance on PhoneBenchAgent and open-source benchmarks,
376 as shown in Table 3. DaMo achieves more than 23% (from 44.83% to 68.18%) improvement over
377 the native model (without SFT) on PhoneAgentBench, surpassing both uniform and natural mixture
strategies. When general capabilities are concurrently considered, DaMo enhances domain-specific

378
379
380
381 Table 3: Main results on PhoneAgentBench and open-source benchmarks by using top-1 data mixture
382 to train MLLM, predicted by DaMo on PhoneAgentBench and open-source benchmarks.
383
384
385
386

Method	MT-Plan	APP-Rec	MM-RR	ACU	MM-NER	Mobile-FC	OS Avg.	PAB Avg.	Overall Avg.
w/o SFT	20.00	6.00	65.38	39.18	84.08	54.31	68.77	44.83	54.40
uniform	54.50	56.00	44.62	86.37	81.71	45.92	55.76	61.52	59.22
natural	47.00	46.00	86.15	83.10	79.83	49.88	59.95	65.33	63.18
DML Ye et al. (2024)	52.00	43.00	85.38	85.72	80.01	42.66	65.48	64.80	65.07
DaMo	55.50	51.00	86.15	85.30	83.34	47.79	68.05	68.18	68.13

387
388
389 Table 4: Main results on open-source benchmarks of MLLMs trained by predicted optimal data
390 mixture on open-source benchmarks.
391

Method	BFCL-V3	MME-perception	MME-reasoning	OCRBench	OS Avg.
w/o SFT	29.32	83.82	79.42	82.50	68.77
uniform	34.69	58.63	64.91	64.80	55.76
natural	31.41	75.47	67.01	65.90	59.95
DML Ye et al. (2024)	25.47	83.31	76.34	76.8	65.48
DaMo	43.15	84.53	80.94	83.60	73.06
DaMo (*)	47.43	85.12	82.54	83.90	/

392
393
394
395
396
397
398
399
400
401
402
403
404
405
406
407
408
409
410
411
412
413
414
415
416
417
418
419
420
421
422
423
424
425
426
427
428
429
430
431
432
433
434
435
436
437
438
439
440
441
442
443
444
445
446
447
448
449
450
451
452
453
454
455
456
457
458
459
460
461
462
463
464
465
466
467
468
469
470
471
472
473
474
475
476
477
478
479
480
481
482
483
484
485
486
487
488
489
490
491
492
493
494
495
496
497
498
499
500
501
502
503
504
505
506
507
508
509
510
511
512
513
514
515
516
517
518
519
520
521
522
523
524
525
526
527
528
529
530
531
532
533
534
535
536
537
538
539
540
541
542
543
544
545
546
547
548
549
550
551
552
553
554
555
556
557
558
559
560
561
562
563
564
565
566
567
568
569
570
571
572
573
574
575
576
577
578
579
580
581
582
583
584
585
586
587
588
589
590
591
592
593
594
595
596
597
598
599
600
601
602
603
604
605
606
607
608
609
610
611
612
613
614
615
616
617
618
619
620
621
622
623
624
625
626
627
628
629
630
631
632
633
634
635
636
637
638
639
640
641
642
643
644
645
646
647
648
649
650
651
652
653
654
655
656
657
658
659
660
661
662
663
664
665
666
667
668
669
670
671
672
673
674
675
676
677
678
679
680
681
682
683
684
685
686
687
688
689
690
691
692
693
694
695
696
697
698
699
700
701
702
703
704
705
706
707
708
709
710
711
712
713
714
715
716
717
718
719
720
721
722
723
724
725
726
727
728
729
730
731
732
733
734
735
736
737
738
739
740
741
742
743
744
745
746
747
748
749
750
751
752
753
754
755
756
757
758
759
750
751
752
753
754
755
756
757
758
759
760
761
762
763
764
765
766
767
768
769
770
771
772
773
774
775
776
777
778
779
770
771
772
773
774
775
776
777
778
779
780
781
782
783
784
785
786
787
788
789
780
781
782
783
784
785
786
787
788
789
790
791
792
793
794
795
796
797
798
799
790
791
792
793
794
795
796
797
798
799
800
801
802
803
804
805
806
807
808
809
800
801
802
803
804
805
806
807
808
809
810
811
812
813
814
815
816
817
818
819
810
811
812
813
814
815
816
817
818
819
820
821
822
823
824
825
826
827
828
829
820
821
822
823
824
825
826
827
828
829
830
831
832
833
834
835
836
837
838
839
830
831
832
833
834
835
836
837
838
839
840
841
842
843
844
845
846
847
848
849
840
841
842
843
844
845
846
847
848
849
850
851
852
853
854
855
856
857
858
859
850
851
852
853
854
855
856
857
858
859
860
861
862
863
864
865
866
867
868
869
860
861
862
863
864
865
866
867
868
869
870
871
872
873
874
875
876
877
878
879
870
871
872
873
874
875
876
877
878
879
880
881
882
883
884
885
886
887
888
889
880
881
882
883
884
885
886
887
888
889
890
891
892
893
894
895
896
897
898
899
890
891
892
893
894
895
896
897
898
899
900
901
902
903
904
905
906
907
908
909
900
901
902
903
904
905
906
907
908
909
910
911
912
913
914
915
916
917
918
919
910
911
912
913
914
915
916
917
918
919
920
921
922
923
924
925
926
927
928
929
920
921
922
923
924
925
926
927
928
929
930
931
932
933
934
935
936
937
938
939
930
931
932
933
934
935
936
937
938
939
940
941
942
943
944
945
946
947
948
949
940
941
942
943
944
945
946
947
948
949
950
951
952
953
954
955
956
957
958
959
950
951
952
953
954
955
956
957
958
959
960
961
962
963
964
965
966
967
968
969
960
961
962
963
964
965
966
967
968
969
970
971
972
973
974
975
976
977
978
979
970
971
972
973
974
975
976
977
978
979
980
981
982
983
984
985
986
987
988
989
980
981
982
983
984
985
986
987
988
989
990
991
992
993
994
995
996
997
998
999
990
991
992
993
994
995
996
997
998
999
1000
1001
1002
1003
1004
1005
1006
1007
1008
1009
1000
1001
1002
1003
1004
1005
1006
1007
1008
1009
1010
1011
1012
1013
1014
1015
1016
1017
1018
1019
1010
1011
1012
1013
1014
1015
1016
1017
1018
1019
1020
1021
1022
1023
1024
1025
1026
1027
1028
1029
1020
1021
1022
1023
1024
1025
1026
1027
1028
1029
1030
1031
1032
1033
1034
1035
1036
1037
1038
1039
1030
1031
1032
1033
1034
1035
1036
1037
1038
1039
1040
1041
1042
1043
1044
1045
1046
1047
1048
1049
1040
1041
1042
1043
1044
1045
1046
1047
1048
1049
1050
1051
1052
1053
1054
1055
1056
1057
1058
1059
1050
1051
1052
1053
1054
1055
1056
1057
1058
1059
1060
1061
1062
1063
1064
1065
1066
1067
1068
1069
1060
1061
1062
1063
1064
1065
1066
1067
1068
1069
1070
1071
1072
1073
1074
1075
1076
1077
1078
1079
1070
1071
1072
1073
1074
1075
1076
1077
1078
1079
1080
1081
1082
1083
1084
1085
1086
1087
1088
1089
1080
1081
1082
1083
1084
1085
1086
1087
1088
1089
1090
1091
1092
1093
1094
1095
1096
1097
1098
1099
1090
1091
1092
1093
1094
1095
1096
1097
1098
1099
1100
1101
1102
1103
1104
1105
1106
1107
1108
1109
1100
1101
1102
1103
1104
1105
1106
1107
1108
1109
1110
1111
1112
1113
1114
1115
1116
1117
1118
1119
1110
1111
1112
1113
1114
1115
1116
1117
1118
1119
1120
1121
1122
1123
1124
1125
1126
1127
1128
1129
1120
1121
1122
1123
1124
1125
1126
1127
1128
1129
1130
1131
1132
1133
1134
1135
1136
1137
1138
1139
1130
1131
1132
1133
1134
1135
1136
1137
1138
1139
1140
1141
1142
1143
1144
1145
1146
1147
1148
1149
1140
1141
1142
1143
1144
1145
1146
1147
1148
1149
1150
1151
1152
1153
1154
1155
1156
1157
1158
1159
1150
1151
1152
1153
1154
1155
1156
1157
1158
1159
1160
1161
1162
1163
1164
1165
1166
1167
1168
1169
1160
1161
1162
1163
1164
1165
1166
1167
1168
1169
1170
1171
1172
1173
1174
1175
1176
1177
1178
1179
1170
1171
1172
1173
1174
1175
1176
1177
1178
1179
1180
1181
1182
1183
1184
1185
1186
1187
1188
1189
1180
1181
1182
1183
1184
1185
1186
1187
1188
1189
1190
1191
1192
1193
1194
1195
1196
1197
1198
1199
1190
1191
1192
1193
1194
1195
1196
1197
1198
1199
1200
1201
1202
1203
1204
1205
1206
1207
1208
1209
1200
1201
1202
1203
1204
1205
1206
1207
1208
1209
1210
1211
1212
1213
1214
1215
1216
1217
1218
1219
1210
1211
1212
1213
1214
1215
1216
1217
1218
1219
1220
1221
1222
1223
1224
1225
1226
1227
1228
1229
1220
1221
1222
1223
1224
1225
1226
1227
1228
1229
1230
1231
1232
1233
1234
1235
1236
1237
1238
1239
1230
1231
1232
1233
1234
1235
1236
1237
1238
1239
1240
1241
1242
1243
1244
1245
1246
1247
1248
1249
1240
1241
1242
1243
1244
1245
1246
1247
1248
1249
1250
1251
1252
1253
1254
1255
1256
1257
1258
1259
1250
1251
1252
1253
1254
1255
1256
1257
1258
1259
1260
1261
1262
1263
1264
1265
1266
1267
1268
1269
1260
1261
1262
1263
1264
1265
1266
1267
1268
1269
1270
1271
1272
1273
1274
1275
1276
1277
1278
1279
1270
1271
1272
1273
1274
1275
1276
1277
1278
1279
1280
1281
1282
1283
1284
1285
1286
1287
1288
1289
1280
1281
1282
1283
1284
1285
1286
1287
1288
1289
1290
1291
1292
1293
1294
1295
1296
1297
1298
1299
1290
1291
1292
1293
1294
1295
1296
1297
1298
1299
1300
1301
1302
1303
1304
1305
1306
1307
1308
1309
1300
1301
1302
1303
1304
1305
1306
1307
1308
1309
1310
1311
1312
1313
1314
1315
1316
1317
1318
1319
1310
1311
1312
1313
1314
1315
1316
1317
1318
1319
1320
1321
1322
1323
1324
1325
1326
1327
1328
1329
1320
1321
1322
1323
1324
1325
1326
1327
1328
1329
1330
1331
1332
1333
1334
1335
1336
1337
1338
1339
1330
1331
1332
1333
1334
1335
1336
1337
1338
1339
1340
1341
1342
1343
1344
1345
1346
1347
1348
1349
1340
1341
1342
1343
1344
1345
1346
1347
1348
1349
1350
1351
1352
1353
1354
1355
1356
1357
1358
1359
1350
1351
1352
1353
1354
1355
1356
1357
1358
1359
1360
1361
1362
1363
1364
1365
1366
1367
1368
1369
1360
1361
1362
1363
1364
1365
1366
1367
1368
1369
1370
1371
1372
1373
1374
1375
1376
1377
1378
1379
1370
1371
1372
1373
1374
1375
1376
1377
1378
1379
1380
1381
1382
1383
1384
1385
1386
1387
1388
1389
1380
1381
1382
1383
1384
1385
1386
1387
1388
1389
1390
1391
1392
1393
1394
1395
1396
1397
1398
1399
1400
1401
1402
1403
1404
1405
1406
1407
1408
1409
1400
1401
1402
1403
1404
1405
1406
1407
1408
1409
1410
1411
1412
1413
1414
1415
1416
1417
1418
1419
1420
1421
1422
1423
1424
1425
1426
1427
1428
1429
1430
1431
1432
1433
1434
1435
1436
1437
1438
1439
1430
1431
1432
1433
1434
1435
1436
1437
1438
1439
1440
1441
1442
1443
1444
1445
1446
1447
1448
1449
1440
1441
1442
1443
1444
1445
1446
1447
1448
1449
1450
1451

We randomly selected a subset of data mixtures from the training and extrapolation samples of the original DaMo and used them to train the new model. As shown in the upper panel of Fig. 5, the Pearson correlation coefficients (r) are generally above 0.75, demonstrating the robust cross-model applicability of DaMo. This suggests that optimal mixtures identified for the base model likely remain near-optimal for the target models.

Due to the varying capabilities across different models, directly transferring DaMo to other models introduces prediction biases. Therefore, we regard DaMo as a model-agnostic predictor: for a new model, we train 20 calibration samples to fit a linear layer that compensates for model discrepancies. The linear-mapped DaMo is defined as $g = f(\cdot) \mathbf{w} + b$ (see details in Appendix C). As shown in the bottom panel of Fig. 5, after applying this linear mapping, the discrepancies between models are reduced, leading to a further enhancement in correlation with r increasing to above 0.9.

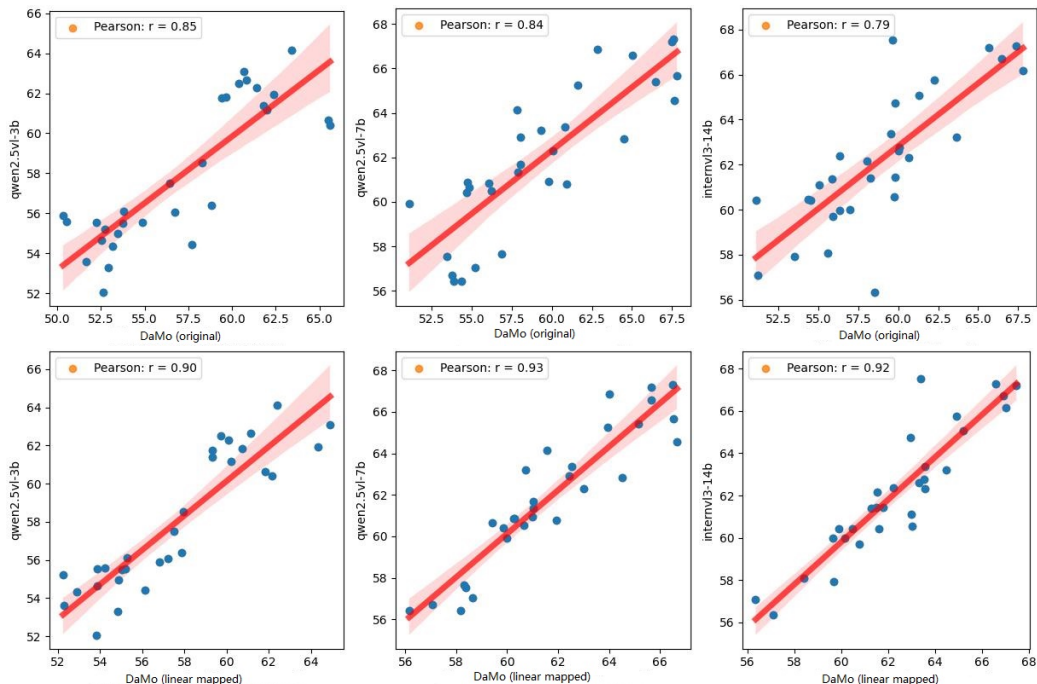


Figure 5: Scalability Analysis. Top: Scatter plot comparing the predicted overall average scores by the original DaMo against the actual scores of target models. Bottom: Apply linear-mapped correction to DaMo.

We performed training and evaluation on the new models using the optimal data mixture predicted by DaMo. As shown in Table 5, directly applying the original DaMo achieves competitive overall average scores, demonstrating the stable transferability of DaMo. Using the linear-mapped DaMo, the scores can be further improved, indicating that the linear mapping mitigates differences in model capabilities and better aligns DaMo with target models.

6 CONCLUSION

In this paper, we present the Data Mixing Optimizer (DaMo) to optimize data mixtures in multitask fine-tuning of multimodal large language models. By introducing downstream task performance prediction with neural network-based modeling, DaMo can predict model performance for any given data mixture. To support comprehensive evaluation, we introduce PhoneAgentBench for evaluation of multimodal large language models on phone agentic tasks. Moreover, DaMo can be extended to other models and tasks. Experimental results demonstrate the efficacy of DaMo not only on PhoneAgentBench, but also on general benchmarks, outperforming the state-of-the-art methods.

486 REFERENCES
487

488 Abhishek Shrivastava. sentiment-analysis-dataset. [https://www.kaggle.com/datasets/](https://www.kaggle.com/datasets/abhi8923shriv/sentiment-analysis-dataset)
489 abhi8923shriv/sentiment-analysis-dataset, 2023. Accessed: 2025-03-12.

490 Josh Achiam, Steven Adler, Sandhini Agarwal, Lama Ahmad, Ilge Akkaya, Florencia Leoni Aleman,
491 Diogo Almeida, Janko Altenschmidt, Sam Altman, Shyamal Anadkat, et al. Gpt-4 technical report.
492 *arXiv preprint arXiv:2303.08774*, 2023.

493 Alon Albalak, Liangming Pan, Colin Raffel, and William Yang Wang. Efficient online data mixing
494 for language model pre-training. *arXiv preprint arXiv:2312.02406*, 2023.

495 Shuai Bai, Keqin Chen, Xuejing Liu, Jialin Wang, Wenbin Ge, Sibo Song, Kai Dang, Peng Wang,
496 Shijie Wang, Jun Tang, et al. Qwen2. 5-vl technical report. *arXiv preprint arXiv:2502.13923*,
497 2025.

498 Kinjal Basu. Bridging knowledge gaps in llms via function calls. In *Proceedings of the 33rd ACM
499 International Conference on Information and Knowledge Management*, pp. 5556–5557, 2024.

500 David Castillo-Bolado, Joseph Davidson, Finlay Gray, and Marek Rosa. Beyond prompts: Dynamic
501 conversational benchmarking of large language models, 2024. URL <https://arxiv.org/abs/2409.20222>.

502 Mingyang Chen, Haoze Sun, Tianpeng Li, Fan Yang, Hao Liang, Keer Lu, Bin Cui, Wentao Zhang,
503 Zhenan Zhou, and Weipeng Chen. Facilitating multi-turn function calling for llms via compositional
504 instruction tuning. *arXiv preprint arXiv:2410.12952*, 2024a.

505 Zehui Chen, Weihua Du, Wenwei Zhang, Kuikun Liu, Jiangning Liu, Miao Zheng, Jingming Zhuo,
506 Songyang Zhang, Dahua Lin, Kai Chen, et al. T-eval: Evaluating the tool utilization capability of
507 large language models step by step. *arXiv preprint arXiv:2312.14033*, 2023.

508 Zhe Chen, Weiyun Wang, Yue Cao, Yangzhou Liu, Zhangwei Gao, Erfei Cui, Jinguo Zhu, Shenglong
509 Ye, Hao Tian, Zhaoyang Liu, et al. Expanding performance boundaries of open-source multimodal
510 models with model, data, and test-time scaling. *arXiv preprint arXiv:2412.05271*, 2024b.

511 Kanzhi Cheng, Qiushi Sun, Yougang Chu, Fangzhi Xu, Yantao Li, Jianbing Zhang, and Zhiyong Wu.
512 Seeclick: Harnessing gui grounding for advanced visual gui agents. *arXiv preprint arXiv:2401.10935*, 2024.

513 Chaoyou Fu, Peixian Chen, Yunhang Shen, Yulei Qin, Mengdan Zhang, Xu Lin, Jinrui Yang, Xiaowu
514 Zheng, Ke Li, Xing Sun, et al. Mme: A comprehensive evaluation benchmark for multimodal
515 large language models. *arXiv preprint arXiv:2306.13394*, 2023.

516 Longxi Gao, Li Zhang, Shihe Wang, Shangguang Wang, Yuanchun Li, and Mengwei Xu. Mobile-
517 views: A large-scale mobile gui dataset. *arXiv preprint arXiv:2409.14337*, 2024.

518 Ce Ge, Zhijian Ma, Daoyuan Chen, Yaliang Li, and Bolin Ding. Bimix: Bivariate data mixing law
519 for language model pretraining. *arXiv preprint arXiv:2405.14908*, 2024.

520 Longling Geng and Edward Y Chang. Realm-bench: A real-world planning benchmark for llms and
521 multi-agent systems. *arXiv preprint arXiv:2502.18836*, 2025.

522 Aaron Grattafiori, Abhimanyu Dubey, Abhinav Jauhri, Abhinav Pandey, Abhishek Kadian, Ahmad
523 Al-Dahle, Aiesha Letman, Akhil Mathur, Alan Schelten, Alex Vaughan, et al. The llama 3 herd of
524 models. *arXiv preprint arXiv:2407.21783*, 2024.

525 Shuhao Gu, Jialing Zhang, Siyuan Zhou, Kevin Yu, Zhaohu Xing, Liangdong Wang, Zhou Cao,
526 Jintao Jia, Zhuoyi Zhang, Yixuan Wang, Zhenchong Hu, Bo-Wen Zhang, Jijie Li, Dong Liang,
527 Yingli Zhao, Yulong Ao, Yaoqi Liu, Fangxiang Feng, and Guang Liu. Infinity-mm: Scaling
528 multimodal performance with large-scale and high-quality instruction data, 2024. URL <https://arxiv.org/abs/2410.18558>.

529 Hamed Rahimi. Sujetfinancevision10k. [https://huggingface.co/datasets/](https://huggingface.co/datasets/sujet-ai/Sujet-Finance-Vision-10k)
530 sujet-ai/Sujet-Finance-Vision-10k, 2024. Accessed: 2025-03-12.

540 Chen Huang, Shuangfei Zhai, Walter Talbott, Miguel Angel Bautista, Shih-Yu Sun, Carlos Guestrin,
 541 and Josh Susskind. Addressing the loss-metric mismatch with adaptive loss alignment, 2019. URL
 542 <https://arxiv.org/abs/1905.05895>.

543 Tim Ingold. *The perception of the environment: essays on livelihood, dwelling and skill*. routledge,
 544 2021.

545 Berivan Isik, Natalia Ponomareva, Hussein Hazimeh, Dimitris Paparas, Sergei Vassilvitskii, and
 546 Sanmi Koyejo. Scaling laws for downstream task performance of large language models. In *ICLR*
 547 2024 Workshop on Mathematical and Empirical Understanding of Foundation Models, 2024.

548 Nathan Lambert, Jacob Morrison, Valentina Pyatkin, Shengyi Huang, Hamish Ivison, Faeze Brahman,
 549 Lester James V Miranda, Alisa Liu, Nouha Dziri, Shane Lyu, et al. T\ ulu 3: Pushing frontiers in
 550 open language model post-training. *arXiv preprint arXiv:2411.15124*, 2024.

551 Hao Li, Chenghao Yang, An Zhang, Yang Deng, Xiang Wang, and Tat-Seng Chua. Hello again!
 552 llm-powered personalized agent for long-term dialogue. *arXiv preprint arXiv:2406.05925*, 2024a.

553 Kaixin Li, Ziyang Meng, Hongzhan Lin, Ziyang Luo, Yuchen Tian, Jing Ma, Zhiyong Huang, and
 554 Tat-Seng Chua. Screenspot-pro: Gui grounding for professional high-resolution computer use.
 555 *arXiv preprint arXiv:2504.07981*, 2025.

556 Lingyu Li, Yixu Wang, Haiquan Zhao, Shuqi Kong, Yan Teng, Chunbo Li, and Yingchun Wang.
 557 Reflection-bench: probing ai intelligence with reflection. *arXiv preprint arXiv:2410.16270*, 2024b.

558 Minghao Li, Yingxiu Zhao, Bowen Yu, Feifan Song, Hangyu Li, Haiyang Yu, Zhoujun Li, Fei Huang,
 559 and Yongbin Li. Api-bank: A comprehensive benchmark for tool-augmented llms, 2023. URL
 560 <https://arxiv.org/abs/2304.08244>.

561 Liang Xu. Superclue-agent. <https://github.com/CLUEbenchmark/SuperCLUE-Agent>, 2024. Accessed: 2025-03-12.

562 Xiao Liu, Hao Yu, Hanchen Zhang, Yifan Xu, Xuanyu Lei, Hanyu Lai, Yu Gu, Hangliang Ding,
 563 Kaiwen Men, Kejuan Yang, et al. Agentbench: Evaluating llms as agents. *arXiv preprint arXiv:2308.03688*, 2023.

564 Xiao Liu, Tianjie Zhang, Yu Gu, Iat Long Iong, Yifan Xu, Xixuan Song, Shudan Zhang, Hanyu Lai,
 565 Xinyi Liu, Hanlin Zhao, et al. Visualagentbench: Towards large multimodal models as visual
 566 foundation agents. *arXiv preprint arXiv:2408.06327*, 2024a.

567 Yanming Liu, Xinyue Peng, Jiannan Cao, Shi Bo, Yuwei Zhang, Xuhong Zhang, Sheng Cheng, Xun
 568 Wang, Jianwei Yin, and Tianyu Du. Tool-planner: Task planning with clusters across multiple
 569 tools. *arXiv preprint arXiv:2406.03807*, 2024b.

570 Yuliang Liu, Zhang Li, Mingxin Huang, Biao Yang, Wenwen Yu, Chunyuan Li, Xu-Cheng Yin,
 571 Cheng-Lin Liu, Lianwen Jin, and Xiang Bai. Ocrbench: on the hidden mystery of ocr in large
 572 multimodal models. *Science China Information Sciences*, 67(12), December 2024c. ISSN
 573 1869-1919. doi: 10.1007/s11432-024-4235-6. URL <http://dx.doi.org/10.1007/s11432-024-4235-6>.

574 Pan Lu, Swaroop Mishra, Tanglin Xia, Liang Qiu, Kai-Wei Chang, Song-Chun Zhu, Oyvind Tafjord,
 575 Peter Clark, and Ashwin Kalyan. Learn to explain: Multimodal reasoning via thought chains for
 576 science question answering. *Advances in Neural Information Processing Systems*, 35:2507–2521,
 577 2022.

578 Grégoire Mialon, Clémentine Fourrier, Craig Swift, Thomas Wolf, Yann LeCun, and Thomas Scialom.
 579 Gaia: a benchmark for general ai assistants, 2023. URL <https://arxiv.org/abs/2311.12983>.

580 Paul Michel, Sebastian Ruder, and Dani Yogatama. Balancing average and worst-case accuracy in
 581 multitask learning. *arXiv: Learning, arXiv: Learning*, Oct 2021.

582 minyang. invoices-and-receipts_ocr_v1. https://huggingface.co/datasets/mychen76/invoices-and-receipts_ocr_v1, 2024. Accessed: 2025-03-12.

594 Niccolò Zanichelli. arxiv-ocr-v0.1.2. https://huggingface.co/datasets/nz_arxiv-ocr-v0.1.2, 2024. Accessed: 2025-03-12.

595

596

597 Haojie Pan, Zepeng Zhai, Hao Yuan, Yaojia Lv, Ruiji Fu, Ming Liu, Zhongyuan Wang, and Bing Qin.

598 Kwaiagents: Generalized information-seeking agent system with large language models. *arXiv*

599 *preprint arXiv:2312.04889*, 2023.

600 qgyd2021. chinese_ner_sft. https://huggingface.co/datasets/qgyd2021_chinese_ner_sft, 2024a. Accessed: 2025-03-12.

601

602

603 qgyd2021. few_shot_ner_sft. https://huggingface.co/datasets/qgyd2021_few_shot_ner_sft, 2024b. Accessed: 2025-03-12.

604

605 Yujia Qin, Shihao Liang, Yining Ye, Kunlun Zhu, Lan Yan, Yaxi Lu, Yankai Lin, Xin Cong, Xiangru

606 Tang, Bill Qian, Sihan Zhao, Lauren Hong, Runchu Tian, Ruobing Xie, Jie Zhou, Mark Gerstein,

607 Dahai Li, Zhiyuan Liu, and Maosong Sun. Toollm: Facilitating large language models to master

608 16000+ real-world apis, 2023. URL <https://arxiv.org/abs/2307.16789>.

609

610 Shiori Sagawa, PangWei Koh, Tatsunori Hashimoto, and Percy Liang. Distributionally robust neural

611 networks. *International Conference on Learning Representations, International Conference on*

612 *Learning Representations*, Apr 2020.

613 shibing624. sharegpt_gpt4. https://huggingface.co/datasets/shibing624_sharegpt_gpt4, 2023. Accessed: 2025-03-12.

614

615 Chan Hee Song, Jiaman Wu, Clayton Washington, Brian M Sadler, Wei-Lun Chao, and Yu Su.

616 Llm-planner: Few-shot grounded planning for embodied agents with large language models. In

617 *Proceedings of the IEEE/CVF international conference on computer vision*, pp. 2998–3009, 2023.

618

619 Karthik Valmeekam, Matthew Marquez, Alberto Olmo, Sarath Sreedharan, and Subbarao Kambham-

620 pati. Planbench: An extensible benchmark for evaluating large language models on planning and

621 reasoning about change. *Advances in Neural Information Processing Systems*, 36:38975–38987,

622 2023.

623 Xuehui Wang, Zhenyu Wu, JingJing Xie, Zichen Ding, Bowen Yang, Zehao Li, Zhaoyang Liu,

624 Qingyun Li, Xuan Dong, Zhe Chen, et al. Mmbench-gui: Hierarchical multi-platform evaluation

625 framework for gui agents. *arXiv preprint arXiv:2507.19478*, 2025.

626

627 Yiqi Wang, Wentao Chen, Xiaotian Han, Xudong Lin, Haiteng Zhao, Yongfei Liu, Bohan Zhai, Jianbo

628 Yuan, Quanzeng You, and Hongxia Yang. Exploring the reasoning abilities of multimodal large

629 language models (mllms): A comprehensive survey on emerging trends in multimodal reasoning.

630 *arXiv preprint arXiv:2401.06805*, 2024.

631 Sewall Wright. Correlation and causation. *Journal of agricultural research*, 20(7):557, 1921.

632

633 Yuxin Xiao, Shujian Zhang, Wenxuan Zhou, Marzyeh Ghassemi, and Sanqiang Zhao. Sftmix:

634 Elevating language model instruction tuning with mixup recipe. *arXiv preprint arXiv:2410.05248*,

635 2024.

636 Sang Michael Xie, Hieu Pham, Xuanyi Dong, Nan Du, Hanxiao Liu, Yifeng Lu,

637 Percy S Liang, Quoc V Le, Tengyu Ma, and Adams Wei Yu. Doremi: Optimiz-

638 ing data mixtures speeds up language model pretraining. In A. Oh, T. Naumann,

639 A. Globerson, K. Saenko, M. Hardt, and S. Levine (eds.), *Advances in Neural In-*

640 *formation Processing Systems*, volume 36, pp. 69798–69818. Curran Associates, Inc.,

641 2023a. URL https://proceedings.neurips.cc/paper_files/paper/2023/file/dcba6be91359358c2355cd920da3fcbd-Paper-Conference.pdf.

642

643 Sang Michael Xie, Hieu Pham, Xuanyi Dong, Nan Du, Hanxiao Liu, Yifeng Lu, Percy S Liang,

644 Quoc V Le, Tengyu Ma, and Adams Wei Yu. Doremi: Optimizing data mixtures speeds up language

645 model pretraining. *Advances in Neural Information Processing Systems*, 36:69798–69818, 2023b.

646

647 Shiming Xie, Hong Chen, Fred Yu, Zeye Sun, and Xiuyu Wu. Minor sft loss for llm fine-tune to

increase performance and reduce model deviation. *arXiv preprint arXiv:2408.10642*, 2024.

648 Fanjia Yan, Huanzhi Mao, Charlie Cheng-Jie Ji, Tianjun Zhang, Shishir G. Patil, Ion Stoica, and
649 Joseph E. Gonzalez. Berkeley function calling leaderboard. 2024.
650

651 Jiasheng Ye, Peiju Liu, Tianxiang Sun, Jun Zhan, Yunhua Zhou, and Xipeng Qiu. Data mixing
652 laws: Optimizing data mixtures by predicting language modeling performance. *arXiv preprint*
653 *arXiv:2403.16952*, 2024.

654 Jiakang Yuan, Tianshuo Peng, Yilei Jiang, Yiting Lu, Renrui Zhang, Kaituo Feng, Chaoyou Fu,
655 Tao Chen, Lei Bai, Bo Zhang, et al. Mme-reasoning: A comprehensive benchmark for logical
656 reasoning in mllms. *arXiv preprint arXiv:2505.21327*, 2025.
657

658 Ruijing Yuan, Shichao Sun, Yongqi Li, Zili Wang, Ziqiang Cao, and Wenjie Li. Personalized large
659 language model assistant with evolving conditional memory. *arXiv preprint arXiv:2312.17257*,
660 2023.

661 Jin Zhang, Jianyang Xue, and Bochao Cao. Improving agent performance in fluid environments by
662 perceptual pretraining. *Physics of Fluids*, 36(12), 2024.

663 Jinguo Zhu, Weiyun Wang, Zhe Chen, Zhaoyang Liu, Shenglong Ye, Lixin Gu, Hao Tian, Yuchen
664 Duan, Weijie Su, Jie Shao, et al. Internvl3: Exploring advanced training and test-time recipes for
665 open-source multimodal models. *arXiv preprint arXiv:2504.10479*, 2025.
666

667 Tong Zhu, Daize Dong, Xiaoye Qu, Jiacheng Ruan, Wenliang Chen, and Yu Cheng. Dynamic data
668 mixing maximizes instruction tuning for mixture-of-experts. *arXiv preprint arXiv:2406.11256*,
669 2024.

670

671

672

673

674

675

676

677

678

679

680

681

682

683

684

685

686

687

688

689

690

691

692

693

694

695

696

697

698

699

700

701

702 A DETAILS OF EXPERIMENTS SETTING
703704 A.1 IMPLEMENT DETAILS
705

706 We applied a series of experiments to verify the effectiveness of DaMo. Initially, we conducted
707 training and evaluation on InternVL2.5-4B Chen et al. (2024b) to obtain fitting samples for the MLP.
708 Specifically, we first sampled 250 random data mixtures \mathbf{p} from \mathcal{P}_{fix} . For each mixture, training was
709 performed on 8 NVIDIA H20 GPUs, and checkpoints were saved at 4 distinct training steps—resulting
710 in a total of 1000 checkpoints. All 1000 checkpoints were then evaluated on downstream tasks, which
711 generated 1000 sample points in the format of $(\mathbf{p}, t, \mathbf{s})$. The hyperparameters for training the MLLM
712 are listed in Table 6.

713 Subsequently, we fitted the MLP on these 1000 sample points. MLP is structured as a two-layer multi-
714 layer perceptron (MLP) built upon `sklearn.MLPRegressor`, where each of the two hidden
715 layers contains 100 neurons. To verify the model’s fitting score, we assessed the coefficient of
716 determination (R^2) Wright (1921) of DaMo via 10-fold cross-validation. More details of MLP are
717 provided in Table 6.

718 Then, we utilized DaMo to predict the downstream task performance of unseen data mixtures.
719 Leveraging the low inference cost of the MLP, we conducted performance predictions for all mixtures
720 $\mathbf{p} \in \mathcal{P}_{\text{fix}}$. Among these, the 50 data mixtures with the optimal predicted performance were selected
721 for further model training and validation, aiming to obtain actual performance metrics.

722 Finally, to verify the scalability of DaMo on other models, we extended DaMo (based on InternVL2.5-
723 4B) to Qwen2.5VL-3B-Instruct, Qwen2.5VL-7B-Instruct Bai et al. (2025), and InternVL3-14B
724 Zhu et al. (2025). For these new models, we trained a small number of random mixtures, analyzed
725 the correlation between DaMo’s predicted performance and the actual training performance, and
726 meanwhile used DaMo to find the optimal mixtures on the new models to verify whether it still
727 maintains competitiveness compared with the baselines.

728
729 Table 6: Hyperparameters of training
730

731	732	733	734	735	736	737	738	739	740	741	742	743	744	745	746	747	748	749	750	751	752	753	754	755	Model	Hyperparameters	setting
						MLLMs	AdamW β_1																			0.9	
							AdamW β_2																		0.95		
							AdamW ϵ																		$1e-6$		
							Max Sequence Length																			16384	
							Batch Size																			16	
							Gradient Accumulation Steps																			8	
							Training Steps																			1440	
							Warmup Steps																			144	
							Peak Learning Rate																			$1e-5$	
							Weight Decay																			0.1	
							Gradient Clipping																			1.0	
						MLP	Input Layer Dimension																		12		
							Hidden Layer 1 Dimension																			100	
							Hidden Layer 2 Dimension																			100	
							Output Layer Dimension																			10	
							Activation Function																			ReLU	
							Optimizer																			Adam	
							Learning Rate																			$1e-6$	
							Training Steps																			10000	

752 A.2 EVALUATION DATASETS
753

754 To guarantee the faithfulness of the proposed PhoneAgentBench, we implemented a rigorous workflow
755 encompassing data filtering, synthetic data generation, and manual verification. Details information
about our evaluation datasets for PhoneAgentBench are as follows.

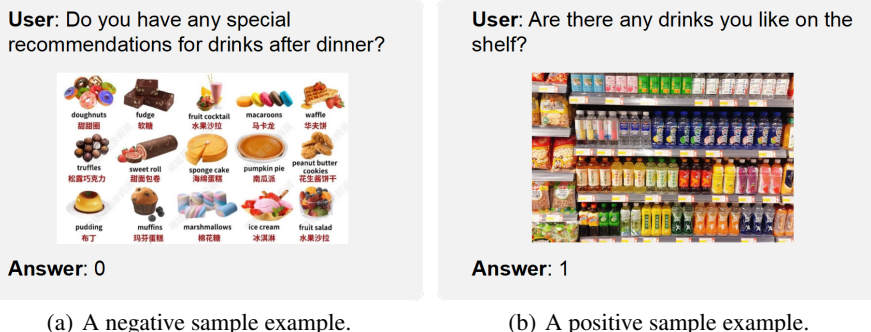
756 A.2.1 MULTIMODAL TASK PLANNING
757758 We introduce the two metrics of complexity and diversity to evaluate the quality of the benchmark for
759 the task planning.

760

- 761 • **Complexity:** The answer of MT-Planning can be viewed as a directed acyclic graph (DAG),
762 where each subtask is a node and the dependency relationship between subtasks are edges.
763 Thus, complexity can be expressed as n_{edge}/n_{node} .
- 764 • **Diversity:** The higher the similarity between queries in a dataset, the lower the diversity of
765 that dataset. We use Rough-L to calculate the similarity between every pair of queries, and
766 diversity can be expressed as $1 - \frac{1}{N(N-1)/2} \sum_{i \neq j} \text{Rough-L}(q_i, q_j)$.

768 Based on this, we compared the data complexity and diversity between MT-Plan and T-Eval planning.
769770 Table 7: benchmark metrics
771

Benchmark	complexity↑	diversity ↑
MT-Plan	0.661	0.82
T-Eval planning Chen et al. (2023)	0.122	0.73

778 A.2.2 MULTIMODAL REFERENCE RESOLUTION
779780 The MultiModal Reference Resolution (MM-RR) task requires the model to determine whether the
781 current question refers to information in the image, which is a binary classification task. As shown in
782 Fig. 6, the question in Fig. 6(a) does not refer to the content in the image, so the answer is 0; while
783 the question in Fig. 6(b) refers to the drinks on the shelf in the image, so the answer is 1.

795 (a) A negative sample example.

796 (b) A positive sample example.

797 Figure 6: Examples of RR dataset.
798800 A.2.3 MULTIMODAL NER
801802 Multimodal NER (MM-NER) benchmark quantitatively measures MLLMs’ ability in understanding
803 and extracting key entities. The dataset comprises 376 image-only samples sourced from Baidu’s
804 publicly available image repositories, where each image underwent a rigorous curation process:
805 professional annotators manually filtered the raw visual data to retain high-quality, clearly discernible
806 images, which were subsequently annotated with precise labels focusing on seven critical entity cate-
807 gories—temporal references, geographical locations, personal identifiers, contact numbers, tracking
808 Number, flight Number, train Number to establish a structured benchmark for multimodal entity
809 recognition. We adopt the entity F1-score as the evaluation metric. Fig. 7 demonstrates time, location
and person extraction from chat logs.



Figure 7: An example of MM-NER dataset.

A.2.4 MOBILE FUNCTION CALL

The Mobile Function Call (Mobile-FC) task is designed to evaluate the ability of MLLMs to call mobile API functions. The task requires the model to select appropriate functions from a given set of application functions to call according to the user's app instruction questions and output the parameters required for the function calls. We define 50 function call interfaces for different scenarios, such as setting an alarm, checking the weather, and setting navigation. The questions in the data are manually constructed by annotators, simulating real-world scenarios of apps on smartphone operating systems and forming complete multi-round dialogues. The evaluation method mainly compares the predicted function names and parameter names with the annotated results. A perfect match scores 1 point; otherwise, 0 points. As shown in the Fig. 8, we define the function name create_alarm for setting an alarm, with the time field as the input parameter.

```

843
844
845
846
847
848
849
850
851
852
853
854
855
856
857
858
859
860
861
862
863

```

User: Set an alarm for 10:00 in the morning.

Answer: create_alarm(time=10:00)

User: An alarm for 03:00.

Answer: create_alarm(time=03:00)

Figure 8: An example of Mobile-FC dataset.

A.2.5 AGENT CONTEXT UNDERSTANDING

The Agent Context Understanding (ACU) task is used to assess the context-aware dialogue comprehension ability of MLLMs. The data is presented in the form of multi-turn conversations (including text and image). The model is required to resolve the anaphoric information in the user's final question based on multi-turn conversations or image information, and output a question that contains no anaphora. As shown in the Fig. 9, the user asks "Do you like his songs?". If no image is provided, the model needs to determine who "he" refers to based on the historical conversation. Otherwise, the model needs to recognize the person in the image. Model's output is a question that contains no referential information. We use the BLEU of the output answer with the reference answer to evaluate task performance, with scores ranging from 0 to 1.

864	User: Do you know Jay Chou?	
865	Assistant: I know Jay Chou. He is a highly influential male pop music singer.	
866		
867		
868	User: Do you like his songs?	
869	Answer: Do you like Jay Chou's songs?	
870		

(a) Pure-text conversation sample.

**User:** Do you like his songs?**Answer:** Do you like Jay Chou's songs?

(b) Multimodal conversation sample.

Figure 9: Examples of ACU dataset.

Table 8: Training dataset sizes.

Dataset	Source	Data size	Dataset	Source	Data size
MMIE	self-built	1.8k	APP-Rec	self-built	22.8k
MMU	self-built	21.1k	RR	self-built	10.5k
TP	self-built	26.8k	FC	self-built	10.4k
ITR	self-built	9.7k	ShareGPT4	open-source	36k
NER	open-source	8k	Infinity-MM	open-source	37.2k
OCR	open-source	33k	SuperCLUE-Agent	open-source	1.5k

A.2.6 APP RECOGNITION

The APP Recognition (APP-Rec) task, similar to the APP-Rec training set, is used to evaluate the ability of MLLMs to identify mobile applications. The model is required to directly output the APP name based on the content of the input mobile APP interface image, as illustrated in the Fig. 11. The performance evaluation is conducted by comparing the overlap between the predicted application name and the annotated result. A correct prediction scores 1 point; otherwise, 0 points.

A.3 TRAINING DATASETS

The open source data includes: ShareGPT4 shibing624 (2023), NER (composed of Chinese-NER-SFT qgyd2021 (2024a), Sentiment-Analysis Abhishek Shrivastava (2023), and Few-Shot-NER-SFT qgyd2021 (2024b)), Infinity-MM Gu et al. (2024), OCR (consisting of Vision-OCR-Financial-Reports-10K Hamed Rahimi (2024), Arxiv-OCR-v0.1-SFT Niccolò Zanichelli (2024) and Invoices-and-Receipts-OCR-v1 minyang (2024)), and SuperCLUE-Agent Liang Xu (2024).

The self-built datasets include MultiModal-Instruction-Evolution (MMIE), APP Recognition (APP-Rec), Reference-Resolution (RR), MultiModal-Understanding (MMU), Function-Calling (FC), Task-Planning (TP), and Image-Text-Relevance (ITR), which are primarily derived from data synthesis and real-world industrial scenarios. The size of samples in all the training data is shown in Table 8.

A.3.1 MULTIMODAL INSTRUCTION EVOLUTION

The Multimodal Instruction Evolution (MMIE) task consists of 1.8K pieces of multimodal question-answering data. As shown in Fig. 10, given an initial query and image with several available tools, the methodology requires the model to generate more sophisticated and diversified questions. The generation pipeline comprises six structured phases:

- **Intent analysis:** Analyze the user’s potential needs from multiple perspectives.
- **Scenario expansion:** Expand the scenario to increase the diversity and complexity of the initial question.
- **Task decomposition:** Decompose the scenario into multiple subtasks which can be executed correctly by provided tools.
- **Raise new question:** Propose a new question based on the expanded scenario and subtasks.

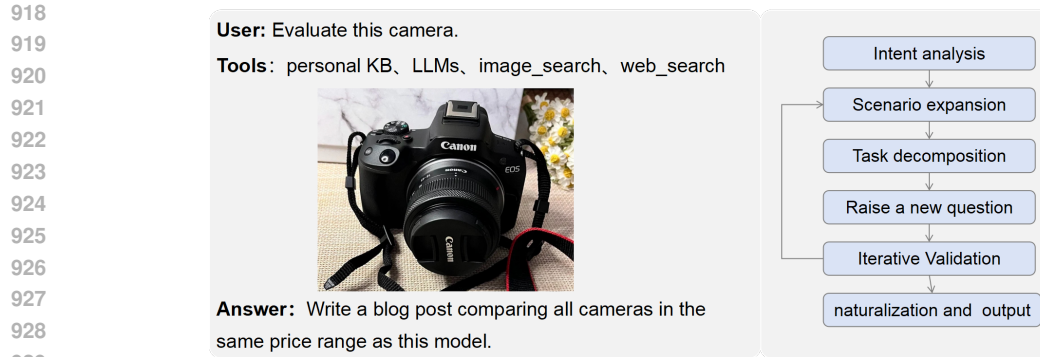


Figure 10: An example of MMIE dataset.

- **Iterative Validation:** Evaluate completeness and complexity, where completeness indicates whether the question adequately covers the steps of the subtasks.
- **Naturalization and output:** Refine questions to be more colloquial and output the final result.

A.3.2 APP RECOGNITION

The APP Recognition (APP-Rec) task consists of 22.8K pieces of multimodal question-answering data, which are composed of images and task instructions. The task requires the model to identify the interface information of mobile apps in the input images and directly output the app names. To obtain diverse app interface data, we install 100 different applications on a mobile phone, such as WeChat, QQ, Little Red Book, Weibo, Alipay, Pinduoduo, Taobao, and TikTok. Annotators are then required to manually capture screenshots of different functional interfaces of each application, which serve as the image source for the APP-Rec task, as illustrated in Fig. 11. The default input task instruction is "Identify which app the screenshot belongs to?", and the answer is the name of the app corresponding to the image.

A.3.3 REFERENCE RESOLUTION

The Reference Resolution (RR) task corresponds to the MM-RR task in Section A.2.2 which contains 10.5K pieces of multimodal question-answering data. We collect various images containing text information from the internet, with sources including academic papers, test questions, news, company official websites, Wikipedia, etc. Annotators design corresponding questions based on the text content in the given images as positive examples, while negative examples are obtained by replacing the images with different types, as shown in the following Fig. 6, which provides one positive and one negative example respectively.

A.3.4 MULTIMODAL UNDERSTANDING

The Multimodal Understanding (MMU) tasks are consistent with ACU tasks in Section A.2.5. It takes the form of multimodal or text-only multi-round dialogues, with 1-4 rounds and a total of 21.1K samples. The images are sourced from publicly available internet data, covering various fields such as people, animals, plants, architecture, and digital products. The dialogue data is manually constructed by annotators based on the given images, focusing on reference problems. The task requires the model to combine the images and historical dialogue content to rewrite the user's final input text. This is achieved by replacing pronouns or supplementing omitted content to make the text semantically complete.

A.3.5 FUNCTION CALLING

The Function Calling (FC) task consists of plain text instructions, which requires selecting appropriate tools from given tool set and filling in correct parameters for executing. The tools involve practical mobile applications such as unit conversion, weather inquiry, time calculation, text creation, recipe

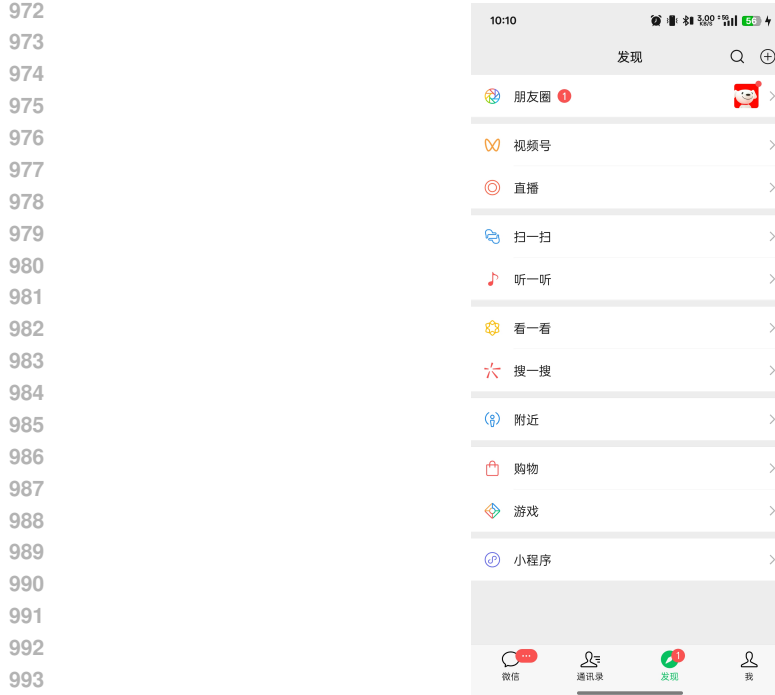


Figure 11: An example of APP-Rec dataset.

search, mobile phone bill inquiry, and other 500 types of useful tools. Notably, 90% of the instructions only require the invocation of a single tool.

Here is an example in Fig. 12: The user inquires how much 500 US dollars is in Japanese yen, and the answer includes thoughts and actions. The thought process briefly outlines the current step, while the action first provides the name of the selected tool and sets the actual parameters in the action input.

```

1004
1005     User: I am planning a trip to Japan next month and wonder how much Japanese yen I can
1006     exchange for 500 USD.
1007
1008     Answer: [
1009         {
1010             "Thought": "Check how many Japanese yen can be exchanged for 500 USD.",
1011             "Action": "exchange_rate",
1012             "Action Input": {
1013                 "money": "500",
1014                 "fromcoin": "USD",
1015                 "tocoins": "JPY"
1016             }
1017         }
1018     ]

```

Figure 12: An output example of FC dataset.

A.3.6 TASK PLANNING

The Task Planning (TP) dataset, also targeting tool calling scenarios, places greater emphasis on multi-stage operations with inter-dependent steps compared to FC. It involves 26.8K pieces of multimodal question-answering data. This dataset requires models to properly decompose complex problems into solvable subtasks while ensuring correct tool selection and execution. In multistep scenarios, managing inter-parameter dependencies becomes critical.

1026
1027
1028
1029
1030
1031
1032
1033
1034
1035
1036
1037
1038
1039
1040
1041
1042
1043
1044
1045
1046
1047
1048
1049
1050
1051
1052
1053
1054
1055
1056
1057
1058
1059
1060
1061
1062
1063
1064
1065
1066
1067
1068
1069
1070
1071
1072
1073
1074
1075
1076
1077
1078
1079

The input is a complex question requiring calling apps on mobile phone. Output contains multistep thinking and actions similar to FC, and symbols start with #E are used to receive parameter for cited in subsequent tasks. (as demonstrated in Fig. 2).

A.3.7 IMAGE-TEXT RELEVANCE

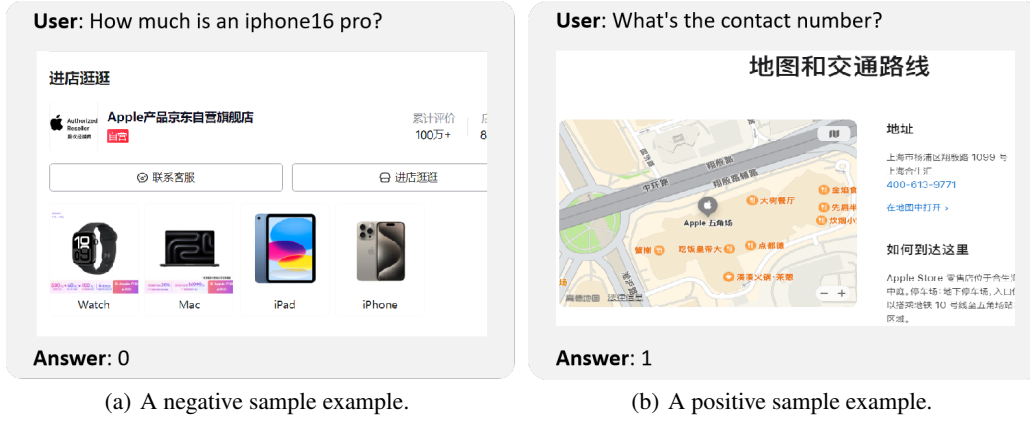


Figure 13: Examples of ITR dataset.

The Image-Text Relevance (ITR) task involves 9.7K pieces of multimodal question-answering data. The task requires the model to analyze the relevance between the question and the image based on the characteristics of the question. If the image is relevant to the question and can be used to answer the user's question, the model should answer 1; otherwise, 0. The images are sourced from publicly available internet data, the same as those used in the MMU task. Annotators manually construct questions related to the image content as positive examples. For example, for images of people, questions about names, works, or family relationships can be asked. Negative examples are constructed by replacing the images with different types, as shown in the following Fig. 13, which presents one positive and one negative example respectively.

B ALGORITHM

Algorithm 1: Algorithm of DaMo

Input: \mathcal{D} : training dataset; \mathcal{D}^{test} : test dataset; θ_0 : initial parameters of MLLM; \mathcal{P} : data mixing space, consisting of data mixture \mathbf{p} ; f_{MLP} : fitted MLP; t : training steps; \mathcal{M} : The data points for fitting MLP, consisting of pairs $\langle(\mathbf{p}, t), \mathbf{s}\rangle$.

Output: θ^* : MLLM trained with the optimal data mixture \mathbf{p}^* .

Initialize $\mathcal{M} \leftarrow \emptyset$

```

Randomly sample a small subset  $\mathcal{P}_{mlp} \subset \mathcal{P}_{fix}$ 
foreach  $\mathbf{p}^i \in \mathcal{P}_{train}$  do
     $\theta_t^i \leftarrow \text{Trainer}(\mathcal{D}, \mathbf{p}^i, t, \theta_0)$ 
     $\mathbf{s}^i \leftarrow \text{Evaluator}(\theta_t^i, \mathcal{D}^{test})$ 
     $\mathcal{M} \leftarrow \mathcal{M} \cup \{(\mathbf{p}^i, t, \mathbf{s}^i)\}$ 
end
 $f_{MLP} \leftarrow \text{fit}(\mathcal{M})$ 
 $\mathbf{p}^*, t^* \leftarrow \arg \max_{\mathbf{p} \in \mathcal{P}_{fix}} f_{MLP}(\mathbf{p}, t)$ 
 $\theta^* \leftarrow \text{Trainer}(\mathcal{D}, \mathbf{p}^*, t^*, \theta_0)$ 
 $\hat{\mathbf{s}} \leftarrow \text{Evaluator}(\theta^*, \mathcal{D}^{test})$ 
return  $\theta^*, \mathbf{s}^*$ 

```

1080 **C EXTENSIBLE VALIDATION**
10811082 We validate the generalizability of DaMo across model families and model sizes (Qwen2.5VL-3B,
1083 Qwen2.5VL-7B, InternVL3-14B) through a two-stage sampling strategy: 1) Random selection from
1084 base model’s experimental mixtures, and 2) Strategic sampling from extrapolated optimal mixtures.
1085 We plot the predicted overall average scores of target models(using the original DaMo) on the x-axis
1086 against the ground-truth overall average scores on the y-axis. If mixture p_i always outperforms
1087 mixture p_j for any i, j across models (Pearson correlation coefficient $r = 1$), it proves that DaMo
1088 has perfect transferability. As shown in the upper panel of Fig. 5, the Pearson correlation coefficients
1089 are consistently above 0.75, demonstrating robust cross-model applicability of DaMo. This suggests
1090 that optimal mixtures identified for base model likely remain near-optimal for target models.1091 Although DaMo demonstrates promising cross-model transferability, model variations still introduce
1092 errors when extrapolating the optimal mixture for target models. To address this, we establish a linear
1093 mapping $g = f()W + b$ between base model’s DaMo F and target model’s optimal law G using 20
1094 calibration samples. This projection improves Pearson correlation to 0.90(bottom panel of Fig. 5),
1095 enabling more precise extrapolation. As Table 5 demonstrates, the linear-mapped DaMo achieve
1096 superior performance compared to direct extrapolation from the base model’s DaMo.1097 **D LIMITATIONS AND FUTURE WORK**
10981100 Our study is grounded in two key assumptions: (1) disregarding sample order within individual
1101 datasets, and (2) maintaining a fixed data mixture ratio throughout training. While recent research
1102 reports the efficacy of multi-stage training and curriculum learning, our preliminary attempts to relax
1103 these assumptions—specifically through dynamic data mixture adjustments—remain exploratory.
1104 We have yet to establish a systematic methodology for extrapolating optimal dynamic mixtures or
1105 quantify the computational costs and performance gains relative to fixed data mixture.1106 Moving forward, we plan to formalize a framework for dynamic data mixture optimization. This
1107 will involve integrating Monte Carlo Tree Search (MCTS) with reinforcement learning to iteratively
1108 determine stage-specific data mixtures, aiming to extrapolate optimal mixture trajectories that mitigate
1109 task conflict and catastrophic forgetting. Additionally, we propose incorporating sample quality
1110 metrics as input variables for downstream performance prediction, enabling difficulty-aware sampling
1111 during training. Further, we will enhance PhoneAgentBench to better align with the fast-evolving
1112 requirements of on-device AI deployment, ensuring its adaptability to emerging mobile-centric AI
1113 paradigms.1114 **E LLM USAGE**
11151116 In this paper, we used LLMs to polish the content of the main text and appendices.
11171118
1119
1120
1121
1122
1123
1124
1125
1126
1127
1128
1129
1130
1131
1132
1133